A Parallel Implementation of the Clarke-Wright Algorithm on GPUs

Francesca Guerriero[a] and Francesco Paolo Saccomanno[b]
Department of Mechanical, Energy and Management Engineering,
University of Calabria, Ponte Pietro Bucci, 87036 Rende, Italy
{francesca.guerriero, francescopaolo.saccomanno}@unical.it

Keywords: Capacitated Vehicle Routing Problem, CVRP, Clarke-Wright Algorithm, GPU Computing, CUDA, Heuristics.

Abstract: The Clark & Wright (CW) algorithm is a greedy approach, aimed at finding good-quality solutions for the capacitated vehicle routing problem (CVRP). It is the most widely applied heuristic algorithm to solve CVRP due to its simple implementation and effectiveness. In this work, we propose a parallel implementation of the CW algorithm well suited to be executed on GPUs. In order to evaluate the performance of the developed approach, an extensive computational phase has been carried out, by considering a large set of test problems. The results are very encouraging, showing a significant reduction in computational time compared to the sequential version, especially for large-scale networks.

1 INTRODUCTION

The Capacitated Vehicle Routing Problem (CVRP) is a NP-Hard combinatorial optimization problem (Laporte, 1992), which seeks to determine an optimal set of routes for a fleet of vehicles, with limited capacity to deliver goods to customers, while minimizing the total transportation cost. Due to its NP-hard nature, finding exact solutions for large-scale instances is computationally intractable, therefore, optimal solutions can be found only when a limited number of nodes (customers and depot) are considered. For more complex scenarios, heuristics and meta-heuristics have been developed to find approximate optimal solutions, (Accorsi and Vigo, 2021), (Liu et al., 2023). Among these, the Clarke-Wright algorithm (CW) is a greedy approach widely used for its efficiency and effectiveness in addressing the CVRP through a simple approach, (Clarke and Wright, 1964), (Augerat et al., 1995). In particular, it relies on building a list of possible savings, obtained when two routes are merged, followed by iterative merging of routes if the constraints of the problem are satisfied. Despite its simplicity, the CW approach, based on savings, can achieve results within 7% of the optimal value, especially for large instances. In the scientific literature, several authors have proposed improvements to the CW algorithm to enhance its effectiveness or address other variants of the CVRP, (Borčinová, 2022), (Nurcahyo et al., 2023), (Tunnisaki and Sutarman, 2023). Parallel computing systems also offer a viable approach for developing solution methods capable of solving large-scale CVRPs. In this work, we propose a parallel implementation of the basic CW algorithm on GPU.

In what follows, a concise overview of the literature related to the development of parallel approaches to solve the CVRP is provided. Attention is focused on the scientific contributions most relevant to our study. Previous studies have primarily focused on parallelizing existing metaheuristics using GPUs to enhance execution speed. These works used graphics processors to handle specific portions of the code. For example, (Benaini and Berrajaa, 2018) proposed a GPU-accelerated evolutionary genetic algorithm for dynamic vehicle routing problems (DVRP), in which requests can occur later. The proposed approach is able to find good-quality solutions for up to 3,000 nodes. Similarly, (Abdelatti and Sodhi, 2020) parallelized a genetic algorithm with local search strategies. Other works used ant colony optimization (Diego et al., 2012), which determines the solution to the problem by imitating the behavior of certain insects in nature, and local search methods (Luong et al., 2013), which iteratively move from one solution to another in a given neighborhood. Similarly, the local search approach is used in (Schulz, 2013). In particular, the two classical heuristics 2-opt and 3-opt were implemented in parallel on GPUs. The instances considered include CVRP and DVRP

[a] https://orcid.org/0000-0002-3887-1317
[b] https://orcid.org/0000-0002-8807-8659

Guerriero, F. and Saccomanno, F. P.
A Parallel Implementation of the Clarke-Wright Algorithm on GPUs.
DOI: 10.5220/0013138100003893

In *Proceedings of the 14th International Conference on Operations Research and Enterprise Systems (ICORES 2025)*, pages 100-111
ISBN: 978-989-758-732-0; ISSN: 2184-4372

problems, ranging from 57 to 2400 nodes.

In (Jin et al., 2014), a tabu search approach is considered, in which the threads work in parallel for the intensification and diversification phase. The authors have achieved effective results in instances with up to 1,200 nodes.

In (Boschetti et al., 2017), the authors used dynamic programming and a relaxation approach, namely state-space relaxation, to compute the bounds. Since these methods are time-consuming, they developed a GPU computing approach and proved that it is capable of achieving up to 40 times time reduction compared to the sequential version, when solving an instance with 2,000 nodes.

(Benaini et al., 2016) presented a GPU-based heuristic for single and multi-depot VRPs, generating initial solutions in parallel and progressively refining them. Unlike our approach, which directly optimizes the CW algorithm's steps, their method uses GPUs to generate multiple initial solutions and relies on the standard CW algorithm. In subsequent works, (Benaini and Berrajaa, 2016), (Benaini et al., 2017) developed GPU implementations for dynamic request insertion and multi-capacity VRPs, respectively. More recent studies, such as (Yelmewad and Talawar, 2021), have focused on improving the performance of local search heuristics using GPUs.

To the best of our knowledge, the only CUDA-based approach aimed at implementing the basic CW algorithm on GPUs has been presented in (Guerriero and Saccomanno, 2024). This early research addresses the merging of tasks sequentially and focuses on cases with a relatively small number of nodes, primarily due to memory constraints. The present paper addresses these limitations and provides a more efficient parallel version of the CW algorithm.

Contribution and Organization of the Paper. This work focuses on developing the CW heuristic on GPUs to enhance performance. A comparison between the GPU implementation and its CPU counterpart reveals significant speed-ups achieved by the GPU, especially for large-scale instances.

The main contributions of this paper are the following:

- development and testing of a parallel version of CW steps, by exploiting GPU capability;
- design and implementation of CUDA Kernel ad-hoc for the calculation of Distance/Cost Matrix and relative savings;
- implementation of a benchmark system to analyse each step of CW algorithm;
- definition of an approach for reducing in parallel the number of operations to be executed sequentially on the CPU.

The structure of the paper is as follows. Section 2 provides a summary of the steps involved in the CW method, illustrating the process on a toy example. Section 3 outlines the proposed parallel approach. Section 4 focuses on the analysis of the computational results, collected in an extensive experimental phase. The paper concludes with final observations in Section 5.

2 THE CW ALGORITHM

The CW approach can be viewed as divided into four main phases: calculating the distance/cost matrix, calculating the savings list, sorting, and finally merging the routes. The cost calculation is typically based on the Euclidean distance between nodes, but other metrics can be used. Furthermore, distances are usually rounded to the nearest integer in experiments, as floating-point calculations are much slower.

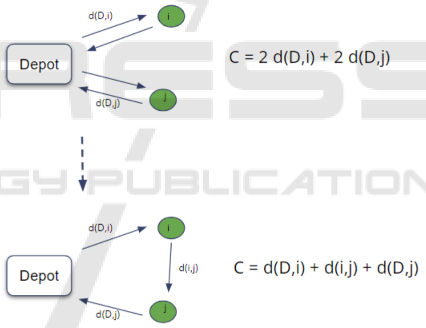

Figure 1: Saving with node i and j.

The list of savings is calculated as the cost reductions that can be achieved when a vehicle transports goods to node i starting from another node j, instead of starting again from the depot d (see Fig. 1):

$$Saving(i,j) = d(D,i) + d(D,j) - d(i,j). \quad (1)$$

In practice, even though it adds a trip and therefore a cost between the nodes i and j, it allows the elimination of two other trips: one between the depot and the nodes i and another between the depot and the node j. Subsequently, before starting route merging, this list of savings is reordered according to decreasing values, allowing the largest savings values to be considered first.

There are two versions of route merging: sequential and parallel. However, these terms do not refer

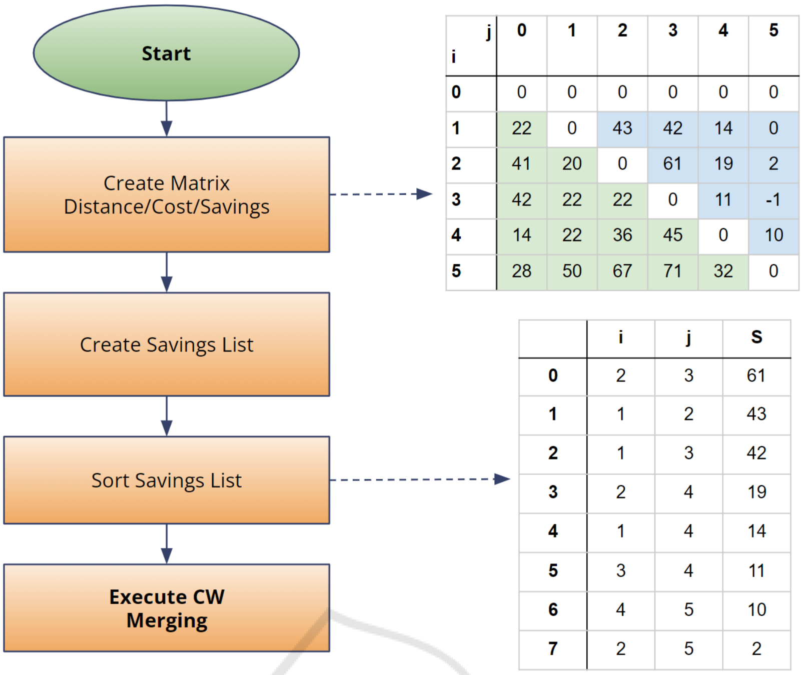

j i	0	1	2	3	4	5
0	0	0	0	0	0	0
1	22	0	43	42	14	0
2	41	20	0	61	19	2
3	42	22	22	0	11	-1
4	14	22	36	45	0	10
5	28	50	67	71	32	0

	i	j	s
0	2	3	61
1	1	2	43
2	1	3	42
3	2	4	19
4	1	4	14
5	3	4	11
6	4	5	10
7	2	5	2

Figure 2: Schematization of the CW algorithm.

to execution on specific hardware, but rather they describe how the elements of the savings list are processed. In the former, the sequential, one route at a time, is completed by sequentially considering the items in the savings list and inserting the nodes that do not violate the constraints. The next route is considered when it is no longer possible to insert further savings into the current one. In the parallel case, instead, an element of the saving list is extracted in sequence and the two indicated routes are merged, always taking into account the constraints. In this case, therefore, during iterations, multiple routes are considered "in parallel".

The performance of the sequential approach presents an average gain compared to the optimal solution of 18%, while in the parallel case, it improves to 7% (Caccetta et al., 2013). For this reason, we will use only the parallel variant of CW in both the CPU and GPU implementations.

In detail, in the parallel case, the merging steps are as follows:

1. The next element of the savings list sorted in descending order is extracted.
2. The constraints are verified: in this work, only the vehicle capacity restrictions are considered, even though it is possible to easily modify the approach to consider time windows or incompatibilities between goods constraints.
3. If the constraints are satisfied, if neither of the two nodes i, j is assigned, a new route is created.
4. Otherwise, the unassigned node is added to the route or the two routes are merged.

To explain how the CW algorithm works, it is useful to consider a toy example made up of six nodes with the following coordinates in the Euclidean space: [10, 20], [10, 40], [30, 30], [-10, 10], [-20, -20] and the depot on [0,0]. The costs, i.e., the distances, are then calculated based on these coordinates (as depicted in Fig. 2). Suppose that the corresponding demand vector is [50, 50, 50, 25, 25] and the vehicle capacity is 100. The first operations to be performed involve calculating the Cost Matrix and the creation and ordering of the Savings List (Fig. 2). Then each link in the savings list is considered: the first one (2,3), since both nodes are unassigned, involves creating a new tour $\{2,3\}$ with a load $50+50=100$, equal to the maximum capacity of the vehicles. After, the links (1,2) and (1,3) are discarded, since nodes 2 and 3 are already present in the tour $\{0,2,3,0\}$, but the vehicle is already full. The iteration proceeds with discarding (2,4), and with the creation of a new tour for the link (1,4) (i.e., $\{0,1,4,0\}$), which reaches a load of 75. Then the link (3,4) is discarded, since the nodes 3 and 4 are already assigned to two different routes. Finally, the link (4,5) is added to obtain from the second tour the new tour $\{0, 1, 4, 5, 0\}$. Obviously, the remaining links (2,5) and (3,5) will be discarded. After processing all the elements of the savings list, the obtained solution (Fig. 3) will consist of only two routes: $\{0,2,3,0\},\{0,1,4,5,0\}$. It is worth noting that, after processing saving (4,5), node 4 becomes internal to the route, allowing us to ignore any subsequent links in the list, where node 4 appears. This key idea will be used in our approach to reduce the remaining items belonging to the savings list, and, in our approach, this reduction will be performed concurrently on GPU.

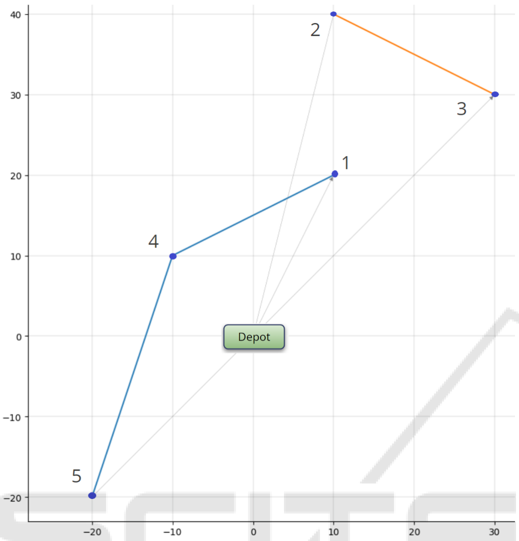

Figure 3: Example with six nodes.

The description provided highlights that although the elements of the savings list require sequential processing, both the computation of the distance/cost matrix and the generation of the savings list can be optimized using parallelization. Consequently, this study aims to implement these steps in parallel by exploiting GPU capabilities and analyzing the potential speed-up over traditional CPU-based processing. As illustrated in the toy example, an alternative technique for the merging phase will also be developed to effectively use the GPU: the list is handled sequentially, but reduced through a parallel method. In the subsequent section, the details of this approach will be clarified.

3 THE CW ALGORITHM ON GPU (CWG)

The purpose of this work is to improve the efficiency of the basic CW approach, by using a GPU. GPUs were created to improve graphics performance, but were later used for mathematical modeling and solving optimization problems. Unlike CPUs, which have a few highly performant cores, GPUs are equipped with thousands of cores capable of performing simpler computations. Among the various usage paradigms, NVidia, one of the GPU brands, introduced the CUDA framework, which allows for abstraction from the physical structure of the graphics card: the functions to be executed in the threads are called kernels, identical for all threads but operating on different data. The various threads are logically grouped into blocks and the blocks are grouped into a grid. The size of the blocks depends on the problem at hand and the resources needed. Each thread uses a private local memory and a shared memory with all other threads in the same block. These memories are fast, but limited, and restrict the maximum number of threads that can be executed in a block. There is also a global memory, which is accessible to all threads in the grid, slower than the previous ones, but generally with capacities reaching up to tens of gigabytes.

CUDA requires the division of processing capacity into blocks made up of t x t threads. A common choice is to use blocks of 32 x 32 or 16 x 16 threads, as these configurations provide a good balance between computational efficiency and compatibility across different GPU architectures. Currently, the maximum number of threads per block in CUDA is 32 x 32 = 1,024. While using a high number of threads might seem advantageous, it can often result in some threads remaining unused. The optimal number of threads per block depends on several factors: the actual number of threads needed for the computation, the available local memory resources per block, and the performance achieved with different block sizes.

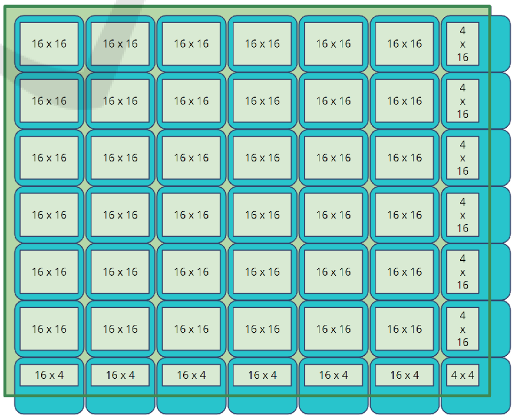

16 x 16	16 x 16	16 x 16	16 x 16	16 x 16	16 x 16	4 x 16
16 x 16	16 x 16	16 x 16	16 x 16	16 x 16	16 x 16	4 x 16
16 x 16	16 x 16	16 x 16	16 x 16	16 x 16	16 x 16	4 x 16
16 x 16	16 x 16	16 x 16	16 x 16	16 x 16	16 x 16	4 x 16
16 x 16	16 x 16	16 x 16	16 x 16	16 x 16	16 x 16	4 x 16
16 x 16	16 x 16	16 x 16	16 x 16	16 x 16	16 x 16	4 x 16
16 x 4	16 x 4	16 x 4	16 x 4	16 x 4	16 x 4	4 x 4

Figure 4: Covering a 100 x 100 matrix using 7 x 7 blocks of 16 x 16 threads.

To better explain the first point, that is, the need to determine the right number of threads to be used, it is useful to consider the example of a matrix with 100 nodes (see Fig. 4), for which the number of operations to be executed (i.e. the cells of the matrix) is 100 x 100 = 10,000. If a block of 16 x 16 threads is chosen, a minimum number of 7 x 7 blocks is needed, for a total of 12,544 threads, therefore the 20.28% of threads remain unused. As illustrated in the figure, the final blocks of threads are only partially utilized, leading to some threads being left idle.

Table 1: Unused threads for different thread block configuration.

Nodes Num.	Block Size			Min Block Numbers			Unused
100	32	x	32	4	x	4	38.96%
300	32	x	32	10	x	10	12.11%
500	32	x	32	16	x	16	4.63%
1000	32	x	32	32	x	32	4.63%
3000	32	x	32	94	x	94	0.53%
5000	32	x	32	157	x	157	0.95%
6000	32	x	32	188	x	188	0.53%
10000	32	x	32	313	x	313	0.32%
20000	32	x	32	626	x	626	0.32%
50000	32	x	32	1563	x	1563	0.06%
100	16	x	16	7	x	7	20.28%
300	16	x	16	19	x	19	2.61%
500	16	x	16	32	x	32	4.63%
1000	16	x	16	63	x	63	1.58%
3000	16	x	16	188	x	188	0.53%
5000	16	x	16	313	x	313	0.32%
6000	16	x	16	376	x	376	0.53%
10000	16	x	16	626	x	626	0.32%
20000	16	x	16	1251	x	1251	0.16%
50000	16	x	16	3126	x	3126	0.06%
100	8	x	8	13	x	13	7.54%
300	8	x	8	38	x	38	2.61%
500	8	x	8	63	x	63	1.58%
1000	8	x	8	126	x	126	1.58%
3000	8	x	8	376	x	376	0.53%
5000	8	x	8	626	x	626	0.32%
6000	8	x	8	751	x	751	0.27%
10000	8	x	8	1251	x	1251	0.16%
20000	8	x	8	2501	x	2501	0.08%
50000	8	x	8	6251	x	6251	0.03%

Tab. 1 shows the amount of unused threads as a function of the number of nodes N and block size. The column “Min Block Numbers” represents the minimum block size of threads to cover the matrix. The last column indicates the percentage of unused threads: this drops below 5% in the case of problems with more than 500 nodes, which are the problems considered in this paper.

The CW algorithm was profiled to identify which specific steps to be implemented in parallel, by using CUDA. Furthermore, this initial analysis allowed us to optimize the various steps of the CPU approach, avoiding the various bottlenecks, including those related to the use of the specific programming language used in the computational phase (that is, Python). This empowers the CPU version efficiently even on medium/large instances, and additionally enables a more effective evaluation of the performance improvement using GPU. As expected, most of the time is spent calculating the distance/cost matrix, creating the savings list, and merging processing in the main loop. For this reason, we have built an ad-hoc CUDA kernel that allows the first two phases of the algorithm to be completed in parallel. Instead, for the sorting phase we relied on the cupy library (https://cupy.dev/) which already offers efficient sorting algorithms based on CUDA. For the last merging phase, we provided a reduction approach that aims to filter the number of savings to analyze, the procedure of which will be described in the next paragraph.

Fig. 5 illustrates the distance/cost matrix to be computed. Each element below the diagonal represents the distance between the nodes, while the elements above the diagonal indicate the possible savings obtained by joining the two nodes i and j. The calculation performed by a thread in a given cell is represented in the figure and reflects the explanations presented in the previous section. From this matrix, the elements above the diagonal are extracted in order to form the savings list (see the lower part of the same figure).

The matrix is computed using a CUDA kernel, which takes care of calculating each of the elements in parallel, therefore, if the number of nodes is N, NxN threads are launched in parallel to compute this matrix: half of these threads are responsible for computing the distances/costs (below the diagonal), and the other half the savings between two nodes.

In practice, in parallel, each created thread takes care of calculating a given element of the matrix using formulas (2) and (1).

$$C = \sqrt{(x_i - x_j)^2 + (y_i - y_j)^2} \qquad (2)$$

Then, the savings list is extracted in the same CUDA kernel which, in a simple way, retrieves the elements above the diagonal and copies them into a contiguous array of savings. The number of threads is equal to the number of possible links between the nodes. Therefore, excluding the links to the depot, it is given by:

$$Link_{i,j} = N * (N-1)/2. \qquad (3)$$

Look Ahead Parallel Reduction (LAPR). In the last stage, the iterations of the CW algorithm cannot be executed in parallel, because the analysis of subsequent savings requires waiting for the previous ones to be processed. A different approach has been developed to utilize the GPU: once a node x is inserted into

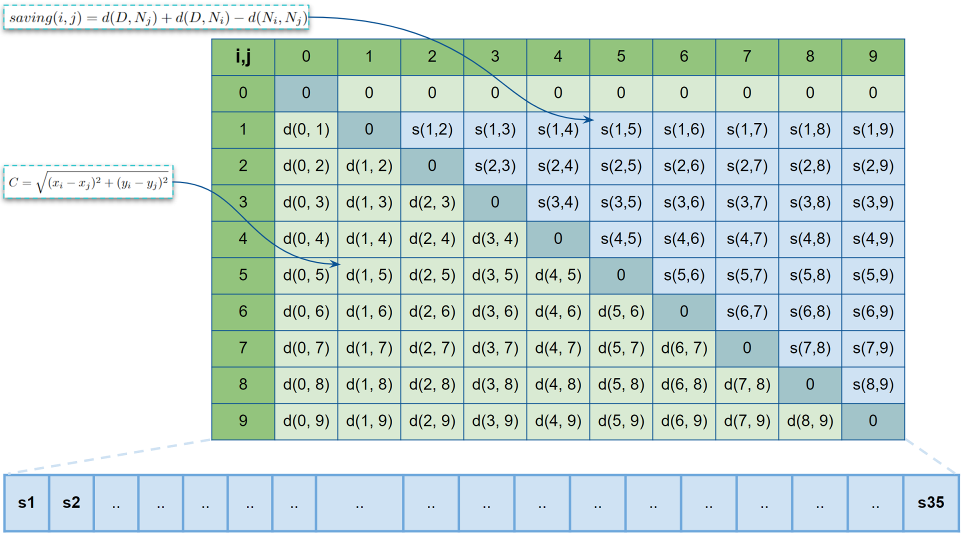

$saving(i,j) = d(D,N_j) + d(D,N_i) - d(N_i,N_j)$

$C = \sqrt{(x_i - x_j)^2 + (y_i - y_j)^2}$

i,j	0	1	2	3	4	5	6	7	8	9
0	0	0	0	0	0	0	0	0	0	0
1	d(0, 1)	0	s(1,2)	s(1,3)	s(1,4)	s(1,5)	s(1,6)	s(1,7)	s(1,8)	s(1,9)
2	d(0, 2)	d(1, 2)	0	s(2,3)	s(2,4)	s(2,5)	s(2,6)	s(2,7)	s(2,8)	s(2,9)
3	d(0, 3)	d(1, 3)	d(2, 3)	0	s(3,4)	s(3,5)	s(3,6)	s(3,7)	s(3,8)	s(3,9)
4	d(0, 4)	d(1, 4)	d(2, 4)	d(3, 4)	0	s(4,5)	s(4,6)	s(4,7)	s(4,8)	s(4,9)
5	d(0, 5)	d(1, 5)	d(2, 5)	d(3, 5)	d(4, 5)	0	s(5,6)	s(5,7)	s(5,8)	s(5,9)
6	d(0, 6)	d(1, 6)	d(2, 6)	d(3, 6)	d(4, 6)	d(5, 6)	0	s(6,7)	s(6,8)	s(6,9)
7	d(0, 7)	d(1, 7)	d(2, 7)	d(3, 7)	d(4, 7)	d(5, 7)	d(6, 7)	0	s(7,8)	s(7,9)
8	d(0, 8)	d(1, 8)	d(2, 8)	d(3, 8)	d(4, 8)	d(5, 8)	d(6, 8)	d(7, 8)	0	s(8,9)
9	d(0, 9)	d(1, 9)	d(2, 9)	d(3, 9)	d(4, 9)	d(5, 9)	d(6, 9)	d(7, 9)	d(8, 9)	0

s1	s2	..	..	..	..	..	..	..	..	..	..	..	..	..	..	..	s35

Figure 5: Representation of operations performed in the CUDA kernel.

a route r, if the node becomes internal to the same route r, or if the route r has reached the maximum capacity C of the vehicle, the node x cannot be considered any more; therefore, we can create a tabu list which contains all nodes that cannot longer be considered. The key idea is to process in parallel the remaining elements of the savings list, on the basis of a "looking ahead" strategy, and to remove all of them that contain nodes belonging to the tabu list, i.e. node that cannot be further inserted or merged in a route. The performance improvements are particularly significant in the case of large-scale instances. In Section 4, the benefits related to the application of this technique, in terms of reduction of the length of the saving list at each iteration, will be highlighted.

Since the merging phase is executed on the CPU, every time the reduction approach is executed on the GPU, a certain overhead is experienced. This limits the possibility of calling the procedure after each node, as the overhead time would exceed the benefit of list reduction. To address this issue, the nodes are inserted into a tabu list and only when a certain number is reached, the parallel reduction procedure is activated. This hyperparameter has been empirically determined, as shown in Section 4.

4 COMPUTATIONAL RESULTS

In order to assess the performance of the proposed approach, computational experiments have been carried out considering *X* instances from (Uchoa et al., 2017) and the *Belgium* sets (Arnold et al., 2019). The choice was made because the first ones are the ones currently most used in evaluating the performance of solution approaches for the CVRP and because they include easy-to-solve instances (starting from 100 nodes, but we have selected those starting from 500), for assessing the overhead of the parallel algorithm, as well as more complicated cases (up to 1,000 nodes). The second dataset (i.e., Belgium dataset) contains test networks with a number of nodes ranging from 3,000 to 30,000. However, due to memory constraints to instantiate matrices and lists, we were able to consider instances of up to 16,000 nodes on CPU. The computational experiments have been carried out by implementing and comparing the following algorithms:

- CWG: the GPU-based parallel implementation of the CW algorithm;
- CWG^f: the first version of CWG introduced in (Guerriero and Saccomanno, 2024). This method is similar to CWG. However, the primary difference lies in its approach of analyzing all items in the savings list, due to the absence of the LAPR procedure;
- CWC: the CPU-based implementation of the CW algorithm;
- PyVRP: the state-of-art algorithm proposed in (Wouda et al., 2024), based on an hybrid genetic search algorithm that combines the global search capabilities of genetic algorithms with local search methods.

The code was developed in Python for both the CPU and the GPU versions, whereas the CUDA kernels were implemented using the NUMBA library. The development environment used is COLAB, an online platform offered by Google for the rapid development of Python-based software. The environment was linked to a local computing system to take advantage of the PC in use equipped of an Intel i9-14900HX 2.2Ghz processor with 24 cores and 64GB of Ram, and a RTX4090 laptop GPU with 16Gb GDDR5 featuring 9728 CUDA cores.

In the subsequent sections, we will investigate the influence of the dimensions of the thread blocks on the performance, the solution quality achieved through the CW method versus the best known solution (BKS), the time comparison against the CWC version, and how the LAPR method affects the number of savings. In addition, a comparison with the state-of-art approach proposed in (Guerriero and Saccomanno, 2024) is also presented.

Impact of Thread Block Size on Performance. The analysis performed in the previous section showed that all threads per block configurations can effectively exploit the number of active threads (see Tab. 1), for the considered instances above 500 nodes, as less than 5% of threads remain inactive.

In the Tab. 2, we report the execution times required by the initial two phases of the CWG algorithm for instances belonging to the Belgium set, with a number of nodes ranging from 3001 to 30001. The columns indicate in order: the instance name, number of nodes, number of threads in a block (TxB), and time of execution as min time (T^{min}), max time (T^{max}) and average time (T^{avg}). The computational results are averaged over 10 runs. This allowed us to determine the minimum, maximum, and average execution times using thread blocks of sizes 8x8, 16x16, and 32x32: although the average value does not differ much, there is a slight advantage for the 16x16 block configuration.

The one with 16x16 threads per block is chosen as it has proved to be the most effective.

Solution Quality Evaluation. In order to evaluate the quality of the solutions determined by the CWG approach, we compared the obtained results with the BKS and with those found by the state-of-the-art PyVRP algorithm, for which a time-limit of 60 seconds has been imposed for instances up to 1001 nodes, and 600 seconds for other instances. In particular, for each test problem, the solution quality gap is evaluated as

$$\delta_{alg1}^{alg2}\% = \frac{(c_{alg1} - c_{alg2})}{c_{alg2}} \times 100,$$

where c represents the cost, and $alg1$ and $alg2$ refer to the approaches under comparison (i.e., CWG, PyVRP, or the BKS).

Table 2: Executions time for different number of threads per block.

Instance	Nodes	TxB	T^{min}	T^{max}	T^{avg}
Leuven1	3001	(8, 8)	0.03	0.12	0.0450
Leuven2	4001	(8, 8)	0.05	0.14	0.0710
Antwerp1	6001	(8, 8)	0.10	0.23	0.1559
Ghent1	10001	(8, 8)	0.33	0.48	0.3990
Ghent2	11001	(8, 8)	0.40	0.56	0.4730
Brussels1	15001	(8, 8)	0.76	0.99	0.9010
Brussels2	16001	(8, 8)	0.92	1.12	1.0290
Flanders1	20001	(8, 8)	1.34	1.56	1.4113
Flanders2	30001	(8, 8)	3.09	3.51	3.2363
				Avg	0.8579
Leuven1	3001	(16, 16)	0.03	0.1	0.0426
Leuven2	4001	(16, 16)	0.05	0.13	0.0705
Antwerp1	6001	(16, 16)	0.10	0.22	0.1499
Ghent1	10001	(16, 16)	0.34	0.48	0.3990
Ghent2	11001	(16, 16)	0.39	0.62	0.4870
Brussels1	15001	(16, 16)	0.77	1.01	0.8600
Brussels2	16001	(16, 16)	0.83	1.09	0.9770
Flanders1	20001	(16, 16)	1.35	1.77	1.4763
Flanders2	30001	(16, 16)	3.00	3.18	3.1188
				Avg	**0.8423**
Leuven1	3001	(32, 32)	0.03	0.11	0.0466
Leuven2	4001	(32, 32)	0.05	0.13	0.0718
Antwerp1	6001	(32, 32)	0.13	0.25	0.1610
Ghent1	10001	(32, 32)	0.36	0.53	0.4360
Ghent2	11001	(32, 32)	0.45	0.58	0.4980
Brussels1	15001	(32, 32)	0.81	0.97	0.8910
Brussels2	16001	(32, 32)	0.91	1.25	1.0310
Flanders1	20001	(32, 32)	1.38	1.66	1.4350
Flanders2	30001	(32, 32)	3.14	3.31	3.2125
				Avg	0.8648

Tab. 3 gives the results for each instance. The first column lists the name of the test problem, followed by the number of nodes in the second column, and the BKS in the third column. The next two columns are related to the PyVRP approach, displaying the solution cost c_{PyVRP} and the solution quality gap $\delta_{PyVRP}^{BKS}\%$ with the respect to the BKS. The final columns summarize the results for the CWG approach, including the cost c_{CWG}, the execution time t_{CWG} and the solution quality gap $\delta_{CWG}^{BKS}\%$ with respect to BKS and $\delta_{CWG}^{PyVRP}\%$ with respect to PyVRP.

For the small-size instances, CWG shows an average GAP of $\delta_{CWG}^{BKS}\% = 5.12\%$ when compared to BKS, and $\delta_{CWG}^{PyVRP}\% = 2.51\%$ in comparison to PyVRP. For larger instances from the Belgium Dataset, CWG increases its performance, with $\delta_{CWG}^{PyVRP}\%$ being 1.60%, 0.53%, and 0.22% for different groups. CWG, on the other hand, has significantly reduced execution times, requiring a maximum of $t_{CWG} = 183$ seconds for the largest scenario considered, which includes

Table 3: Benchmarking Solution Quality.

Instance Name	Nodes	BKS	PyVRP		CWG			
			c_{PyVRP}	$\delta_{Py}^{BKS}\%$	c_{CWG}	t_{CWG}	$\delta_{CWG}^{BKS}\%$	$\delta_{CWG}^{Py}\%$
X-n502-k39	502	69226	69740	0.74%	71388	0.53	3.12%	2.36%
X-n513-k21	513	24201	24562	1.49%	26805	0.41	10.76%	9.13%
X-n524-k153	524	154593	155531	0.61%	163352	0.42	5.67%	5.03%
X-n536-k96	536	94846	96514	1.76%	99872	0.46	5.30%	3.48%
X-n548-k50	548	86700	88390	1.95%	89574	0.45	3.31%	1.34%
X-n561-k42	561	42717	43721	2.35%	45557	0.45	6.65%	4.20%
X-n573-k30	573	50673	51780	2.18%	52565	0.46	3.73%	1.52%
X-n586-k159	586	190316	193405	1.62%	199817	0.54	4.99%	3.32%
X-n599-k92	599	108451	111045	2.39%	113296	0.53	4.47%	2.03%
X-n613-k62	613	59535	60837	2.19%	62829	0.49	5.53%	3.27%
X-n627-k43	627	62164	63523	2.19%	65218	0.52	4.91%	2.67%
X-n641-k35	641	63682	66233	4.01%	67550	0.64	6.07%	1.99%
X-n655-k131	655	106780	107480	0.66%	108353	0.61	1.47%	0.81%
X-n670-k130	670	146332	148413	1.42%	158154	0.63	8.08%	6.56%
X-n685-k75	685	68205	69940	2.54%	71685	0.64	5.10%	2.49%
X-n701-k44	701	81923	84959	3.71%	85589	0.61	4.47%	0.74%
X-n716-k35	716	43373	45238	4.30%	45744	0.53	5.47%	1.12%
X-n733-k159	733	136187	140627	3.26%	139997	0.81	2.80%	-0.45%
X-n749-k98	749	77269	79838	3.32%	79462	0.69	2.84%	-0.47%
X-n766-k71	766	114417	117711	2.88%	119262	0.77	4.23%	1.32%
X-n783-k48	783	72386	75598	4.44%	76566	0.91	5.77%	1.28%
X-n801-k40	801	73305	76321	4.11%	76700	0.86	4.63%	0.50%
X-n819-k171	819	158121	161054	1.85%	166287	0.9	5.16%	3.25%
X-n837-k142	837	193737	198166	2.29%	200443	1.03	3.46%	1.15%
X-n856-k95	856	88965	90453	1.67%	92368	1.05	3.83%	2.12%
X-n876-k59	876	99299	102140	2.86%	102306	0.98	3.03%	0.16%
X-n895-k37	895	53860	56052	4.07%	58614	1.04	8.83%	4.57%
X-n916-k207	916	329179	334298	1.56%	343501	0.97	4.35%	2.75%
X-n936-k151	936	132715	137082	3.29%	146523	1.23	10.40%	6.89%
X-n957-k87	957	85465	87608	2.51%	89212	1.09	4.38%	1.83%
X-n979-k58	979	118976	121788	2.36%	123690	1.27	3.96%	1.56%
X-n1001-k43	1001	72355	75955	4.98%	77377	1.52	6.94%	1.87%
				2.55%			**5.12%**	**2.51%**
Leuven1	3001	192848	200297	3.86%	200790	3.75	4.12%	0.25%
Leuven2	4001	111391	118483	6.37%	124194	3.49	11.49%	4.82%
Antwerp1	6001	477277	497588	4.26%	497009	4.83	4.13%	-0.12%
Antwerp2	7001	291350	312371	7.22%	316878	7.57	8.76%	1.44%
				5.43%			**7.13%**	**1.60%**
Ghent1	10001	469,531	491610	4.70%	488056	14.18	3.95%	-0.72%
Ghent2	11001	257,748	277372	7.61%	283202	15.87	9.88%	2.10%
Brussels1	15001	501,719	533768	6.39%	529846	35.69	5.61%	-0.73%
Brussels2	16001	345,468	373996	8.26%	379516	29.95	9.86%	1.48%
				6.74%			**7.32%**	**0.53%**
Flanders1	20001	7240118	7542347	4.17%	7497837	54.74	3.56%	-0.59%
Flanders2	30001	4373244	4716145	7.84%	4764789	182.57	8.95%	1.03%
				6.01%			**6.26%**	**0.22%**

30K nodes.

The results indicate that the proposed CWG approach is capable of producing solutions of a quality comparable to PyVRP, while offering substantial improvements in terms of computational time.

Time Analysis Against CWC Version. Table 4 presents the results obtained with CWC. In particular, the first column displays the name of the instance, whereas the second gives the number of nodes. The subsequent columns display the total execution time of the CWC approach (T_{CWC}), the time spent creat-

Table 4: Time Analysis against CWC version.

Instance	Nodes	T_{CWC}	T^1_{CWC}	T^2_{CWC}	T^3_{CWC}	T^4_{CWC}	T_{CWG}	T^1_{CWG}	T^2_{CWG}	T^3_{CWG}	T^4_{CWG}	Speed-UP
X-n502-k39	502	1.40	0.77	0.45	0.01	0.17	0.53	0.01	0.00	0.01	0.51	3
X-n513-k21	513	1.58	0.98	0.35	0.01	0.24	0.41	0.01	0.00	0.00	0.40	4
X-n524-k153	524	1.37	0.68	0.41	0.02	0.26	0.42	0.01	0.00	0.00	0.41	3
X-n536-k96	536	1.23	0.69	0.35	0.01	0.18	0.46	0.01	0.00	0.00	0.45	3
X-n548-k50	548	1.36	0.75	0.41	0.01	0.19	0.45	0.01	0.00	0.00	0.44	3
X-n561-k42	561	1.65	0.97	0.46	0.01	0.21	0.45	0.01	0.00	0.00	0.44	4
X-n573-k30	573	1.59	0.84	0.48	0.01	0.26	0.46	0.01	0.00	0.00	0.45	3
X-n586-k159	586	1.61	0.94	0.40	0.01	0.26	0.54	0.01	0.00	0.00	0.53	3
X-n599-k92	599	1.66	0.90	0.47	0.01	0.28	0.53	0.01	0.00	0.00	0.52	3
X-n613-k62	613	1.66	1.00	0.42	0.01	0.23	0.49	0.01	0.00	0.00	0.48	3
X-n627-k43	627	1.77	1.02	0.49	0.01	0.25	0.52	0.01	0.00	0.00	0.51	3
X-n641-k35	641	1.92	1.14	0.52	0.01	0.25	0.64	0.01	0.00	0.00	0.63	3
X-n655-k131	655	2.06	1.15	0.55	0.02	0.34	0.61	0.01	0.00	0.01	0.59	3
X-n670-k130	670	1.91	1.08	0.51	0.01	0.31	0.63	0.01	0.00	0.01	0.61	3
X-n685-k75	685	2.23	1.22	0.60	0.04	0.37	0.64	0.01	0.00	0.01	0.62	3
X-n701-k44	701	2.35	1.42	0.62	0.02	0.29	0.61	0.01	0.00	0.01	0.59	4
X-n716-k35	716	2.77	1.51	0.77	0.04	0.45	0.53	0.01	0.00	0.01	0.51	5
X-n733-k159	733	2.51	1.42	0.68	0.02	0.39	0.81	0.01	0.00	0.01	0.79	3
X-n749-k98	749	2.44	1.44	0.66	0.01	0.33	0.69	0.01	0.00	0.01	0.67	4
X-n766-k71	766	2.45	1.48	0.62	0.02	0.33	0.77	0.01	0.00	0.01	0.75	3
X-n783-k48	783	2.64	1.53	0.71	0.02	0.38	0.91	0.01	0.00	0.01	0.89	3
X-n801-k40	801	2.84	1.55	0.81	0.03	0.45	0.86	0.01	0.00	0.01	0.84	3
X-n819-k171	819	2.88	1.60	0.83	0.02	0.43	0.90	0.01	0.00	0.01	0.88	3
X-n837-k142	837	3.01	1.74	0.79	0.02	0.46	1.03	0.01	0.00	0.01	1.01	3
X-n856-k95	856	3.14	1.74	0.87	0.03	0.50	1.05	0.02	0.00	0.01	1.02	3
X-n876-k59	876	3.53	1.99	0.99	0.03	0.52	0.98	0.01	0.00	0.01	0.96	4
X-n895-k37	895	3.32	1.87	0.92	0.03	0.50	1.04	0.01	0.00	0.01	1.02	3
X-n916-k207	916	3.83	2.14	1.05	0.03	0.61	0.97	0.01	0.00	0.01	0.95	4
X-n936-k151	936	4.17	2.29	1.15	0.03	0.70	1.23	0.01	0.00	0.01	1.21	3
X-n957-k87	957	4.09	2.28	1.17	0.06	0.58	1.09	0.01	0.00	0.01	1.07	4
X-n979-k58	979	4.15	2.42	0.97	0.04	0.72	1.27	0.01	0.00	0.01	1.25	3
X-n1001-k43	1001	4.47	2.62	1.20	0.03	0.62	1.52	0.02	0.00	0.01	1.49	3
Leuven1	3001	47.15	27.00	13.01	0.64	6.50	3.75	0.12	0.00	0.07	3.56	13
Leuven2	4001	84.70	46.48	24.33	1.29	12.60	3.49	0.21	0.00	0.03	3.25	24
Antwerp1	6001	186.33	114.14	46.20	2.87	23.12	4.83	0.34	0.00	0.08	4.41	39
Antwerp2	7001	207.33	120.09	53.91	3.98	29.35	7.57	1.09	0.00	0.12	6.36	27
Ghent1	10001	543.66	305.96	137.03	10.63	90.04	14.18	0.57	0.00	0.20	13.41	38
Ghent2	11001	657.45	370.74	181.01	11.95	93.75	15.87	0.74	0.00	0.57	14.56	41
Brussels1	15001	1073.02	570.40	275.92	25.19	201.51	35.69	1.06	0.00	0.61	34.02	30
Brussels2	16001	1393.93	777.41	373.63	30.97	211.92	29.95	1.11	0.00	0.55	28.29	47
Average		106.83					3.48					**9.10**

ing the distance/cost matrix (T^1_{CWC}), generating the savings list (T^2_{CWC}), ordering (T^3_{CWC}), and executing merge iterations (T^4_{CWC}). Similarly, times for CWG operations on GPU are given (i.e., T_{CWG}, T^1_{CWG}, T^2_{CWG}, T^3_{CWG}, T^4_{CWG}). The last column displays the speed-up achieved by the CWG compared to the CWC, calculated as $\frac{T_{CWC}}{T_{CWG}}$.

The results show the ability of the CWG approach to scale in the calculation of the cost matrix and the savings list. In particular, the higher the number of nodes, the higher the speed-up achieved. For example, for the Brussels2 instance it reduces from 1151.04 seconds (i.e., 777.41 + 373.63 seconds) to 1.11 seconds.

It should be noted that in the case of the CWG approach, the savings list creation time is equal to 0 since this, as we saw in the previous section, is calculated in parallel together with the cost matrix. As expected, the first three phases, being entirely processed on the GPU, benefit from the maximum speed-up. Although the final route merging phase is performed on the CPU, it still achieves significant time improvement due to the reductions provided by the LAPR procedure. For instance, in the Brussels2 case, the total time decreases from 211.92 to 28.29 seconds.

Clearly, the performance improvements of the CWG implementation compared to the CWC version become more significant for the latest set of test problems under consideration. In effect, the real potential of the CWG becomes more evident in these latter instances, characterized by a high number of nodes.

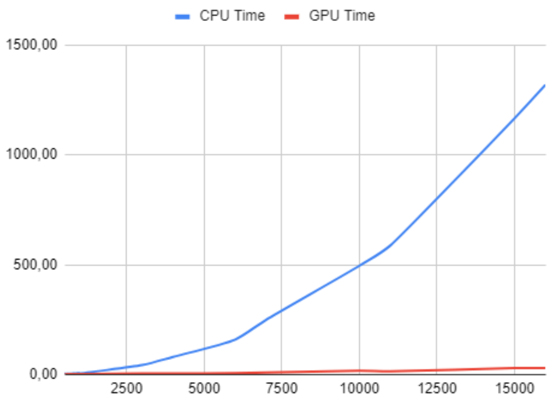

Figure 6: Execution time of CWC (blue) and CWG (red).

Figure 6 shows the execution times as a function of the number of nodes for the CWC (blue), where the trend is exponential, and for the CWG (red), which remains essentially linear.

Impact of LAPR. The table 5 shows the results obtained by applying the LAPR approach. The first two columns indicate the instance name and the number of nodes, respectively. The next two columns are related to the number of entries in the original savings list Len^{Ori} and those belonging to the reduced list Len^{Red}. The last column displays the reduction achieved, determined as

$$\delta_{RA}\% = \frac{Len^{Red}}{Len^{Ori}} \times 100.$$

The computational results underline a substantial reduction. In fact, considering that each node is connected with all other nodes to obtain the savings list, each time a node is excluded, on average, entries equal to the number of nodes are removed from the savings list. This approach required adjusting a hyperparameter that defines how often nodes, present in the tabu list, should activate the reduction procedure. Since the merging is done on the CPU and reduction on the GPU, each time reduction is invoked, necessary overhead must be considered. Empirically, we found that the best result is obtained by filtering the list when the tabu list contains 1,000 nodes.

Table 5: LAPR reduction of savings list.

Instance	Nodes	Len^{Ori}	Len^{Red}	$\delta_{RA}\%$
X-n502-k39	502	125250	23696	19%
X-n513-k21	513	130816	11593	9%
X-n524-k153	524	136503	70336	52%
X-n536-k96	536	142845	46667	33%
X-n548-k50	548	149331	32120	22%
X-n561-k42	561	156520	18518	12%
X-n573-k30	573	163306	27272	17%
X-n586-k159	586	170820	102870	60%
X-n599-k92	599	178503	57547	32%
X-n613-k62	613	186966	27913	15%
X-n627-k43	627	195625	39735	20%
X-n641-k35	641	204480	25929	13%
X-n655-k131	655	213531	76920	36%
X-n670-k130	670	223446	79827	36%
X-n685-k75	685	233586	30928	13%
X-n701-k44	701	244650	37951	16%
X-n716-k35	716	255255	33764	13%
X-n733-k159	733	267546	90159	34%
X-n749-k98	749	279378	58502	21%
X-n766-k71	766	292230	49023	17%
X-n783-k48	783	305371	38183	13%
X-n801-k40	801	319600	35025	11%
X-n819-k171	819	334153	108502	32%
X-n837-k142	837	349030	105944	30%
X-n856-k95	856	365085	46315	13%
X-n876-k59	876	382375	50136	13%
X-n895-k37	895	399171	28040	7%
X-n916-k207	916	418155	176281	42%
X-n936-k151	936	436645	84975	19%
X-n957-k87	957	456490	59367	13%
X-n979-k58	979	477753	66164	14%
X-n1001-k43	1001	499500	39275	8%
Leuven1	3001	4498500	974232	22%
Leuven2	4001	7998000	1092037	14%
Antwerp1	6001	17997000	1187458	7%
Antwerp2	7001	24496500	1498080	6%
Ghent1	10001	49995000	2826278	6%
Ghent2	11001	60494500	1878885	3%
Brussels1	15001	112492500	3336386	3%
Brussels2	16001	127992000	2287755	2%
Flanders1	20001	199990000	5018038	3%
Flanders2	30001	449985000	5022633	1%

Comparison with Previous Approach. Lastly, the Tab. 6 presents a comparative analysis of performance with the algorithm in (Guerriero and Saccomanno, 2024), in eight different instances, selected due to their large number of nodes. The columns represent the instance, the computational time in seconds for both algorithms (T^{f}_{CWG} and T_{CWG}), and the percentage reduction in computational time when using T^{f}_{CWG} compared to T_{CWG}, calculated as

$$\delta_{TR}\% = \left(\frac{T^{f}_{CWG} - T_{CWG}}{T^{f}_{CWG}} \right) \times 100.$$

CWG demonstrates a decrease in time ranging from at least 75% to as much as 93%. Furthermore, as the number of nodes increases, the time reduction becomes more significant, highlighting the impact of the LAPR procedure that is absent in T^{f}_{CWG}. In effect, previous research focused on assessing the viability of running the CW algorithm on GPUs and analyzing the execution times of various steps on both the CPU and GPU. However, that study did not include the development of the LAPR reduction method, thus the route merging phase was quite costly due to the large number of savings to process when dealing with instances that have a high number of nodes.

Table 6: Comparison with (Guerriero and Saccomanno, 2024).

Instance	T^f_{CWG}	T_{CWG}	$\delta_{TR}\%$
L1	15.21	3.75	75.35%
L2	23.40	3.49	85.09%
A1	46.78	4.83	89.68%
A2	72.30	7.57	89.53%
G1	155.66	14.18	90.89%
G2	203.80	15.87	92.21%
B1	393.24	35.69	90.92%
B2	451.05	29.95	93.36%
Average	170.18	14.42	88.38%

5 CONCLUSIONS

In this work, a CWG implementation on GPU of the CW algorithm was proposed. The computational results collected clearly highlight that it is significantly faster than the CWC implementation, especially for large instances. This is due to the parallel processing capabilities of GPUs, which enable efficient execution of the computational steps of the algorithm, leading to substantial speedups.

Comparison with a state-of-the-art PyVRP algorithm, which uses the same initial data structures, indicates that the GPU implementation could significantly improve the performance and scalability of such a solver, particularly in the early stages, therefore suggesting a possible integration of the two approaches. Moreover, by enabling substantial acceleration in the search for an initial solution, albeit not necessarily optimal, this approach can be integrated into other heuristics to quickly provide an initial solution. It can also serve as the basis for an iterative method, aimed at quickly exploring the solution space.

Future research could focus on extending the applicability of GPU-accelerated CW algorithms to more complex VRP variants and exploring their potential for solving related optimization problems across various domains.

For instance, it provides an effective approach for real-time applications needing rapid, nearly optimal vehicle routing solutions. Our findings indicate that the algorithm consistently achieves results within a 7% gap from optimal, thus making it ideal for scenarios where timely decisions are essential. By utilizing the parallel processing power of GPUs, we have accomplished notable speed enhancements, allowing the algorithm to produce high-quality solutions in much less time than standard CPU-based methods. These results underscore the promise of GPU acceleration in addressing complex optimization challenges in dynamic and time-sensitive settings.

REFERENCES

Abdelatti, M. F. and Sodhi, M. S. (2020). An improved gpu-accelerated heuristic technique applied to the capacitated vehicle routing problem. In *Proceedings of the 2020 Genetic and Evolutionary Computation Conference*, GECCO '20, page 663–671, New York, NY, USA. Association for Computing Machinery.

Accorsi, L. and Vigo, D. (2021). A fast and scalable heuristic for the solution of large-scale capacitated vehicle routing problems. *Transportation Science*, 55(4):832–856.

Arnold, F., Gendreau, M., and Sörensen, K. (2019). Efficiently solving very large-scale routing problems. *Computers & Operations Research*, 107:32–42.

Augerat, P., Belenguer, J. M., Benavent, E., Corberan, A., Naddef, D., and Rinaldi, G. (1995). Computational results with a branch and cut code for the capacitated vehicle routing problem. *Computer Science, Mathematics*.

Benaini, A. and Berrajaa, A. (2016). Solving the dynamic vehicle routing problem on gpu. In *2016 3rd International Conference on Logistics Operations Management (GOL)*, pages 1–6.

Benaini, A. and Berrajaa, A. (2018). Genetic algorithm for large dynamic vehicle routing problem on gpu. In *2018 4th International Conference on Logistics Operations Management (GOL)*, pages 1–9.

Benaini, A., Berrajaa, A., and Daoudi, E. M. (2016). Solving the vehicle routing problem on gpu. In El Oualkadi, A., Choubani, F., and El Moussati, A., editors, *Proceedings of the Mediterranean Conference on Information & Communication Technologies 2015*, pages 239–248, Cham. Springer International Publishing.

Benaini, A., Berrajaa, A., and Daoudi, E. M. (2017). Parallel implementation of the multi capacity vrp on gpu. In Rocha, Á., Serrhini, M., and Felgueiras, C., editors, *Europe and MENA Cooperation Advances in Information and Communication Technologies*, pages 353–364, Cham. Springer International Publishing.

Borčinová, Z. (2022). Kernel search for the capacitated vehicle routing problem. *Applied Sciences*, 12(22).

Boschetti, M. A., Maniezzo, V., and Strappaveccia, F. (2017). Route relaxations on gpu for vehicle routing problems. *European Journal of Operational Research*, 258(2):456–466.

Caccetta, L., Alameen, M., and Abdul-Niby, M. (2013). An improved clarke and wright algorithm to solve the capacitated vehicle routing problem. *Engineering, Technology & Applied Science Research*, 3(2):413–415.

Clarke, G. and Wright, J. W. (1964). Scheduling of vehicles from a central depot to a number of delivery points. *Operations research*, 12(4):568–581.

Diego, F. J., Gómez, E. M., Ortega-Mier, M., and García-Sánchez, Á. (2012). Parallel cuda architecture for solving de vrp with aco. In Sethi, S. P., Bogataj, M., and Ros-McDonnell, L., editors, *Industrial Engineering: Innovative Networks*, pages 385–393, London. Springer London.

Guerriero, F. and Saccomanno, F. (2024). Accelerating the clarke-wright algorithm for the capacitated vehicle routing problem using gpus. In *Proceedings of BOS / SOR 2024, Polish Operational and Systems Research Society Conference*, Warsaw.

Jin, J., Crainic, T. G., and Løkketangen, A. (2014). A cooperative parallel metaheuristic for the capacitated vehicle routing problem. *Computers & Operations Research*, 44:33–41.

Laporte, G. (1992). The vehicle routing problem: An overview of exact and approximate algorithms. *European Journal of Operational Research*, 59(3):345–358.

Liu, F., Lu, C., Gui, L., Zhang, Q., Tong, X., and Yuan, M. (2023). Heuristics for vehicle routing problem: A survey and recent advances.

Luong, T. V., Melab, N., and Talbi, E.-G. (2013). Gpu computing for parallel local search metaheuristic algorithms. *IEEE Transactions on Computers*, 62(1):173–185.

Nurcahyo, R., Irawan, D. A., and Kristanti, F. (2023). The effectiveness of the clarke & wright savings algorithm in determining logistics distribution routes (case study pt.xyz). *E3S Web of Conferences*, 426.

Schulz, C. (2013). Efficient local search on the gpu—investigations on the vehicle routing problem. *Journal of Parallel and Distributed Computing*, 73(1):14–31. Metaheuristics on GPUs.

Tunnisaki, F. and Sutarman (2023). Clarke and wright savings algorithm as solutions vehicle routing problem with simultaneous pickup delivery (vrpspd). *Journal of Physics: Conference Series*, 2421(1):012045.

Uchoa, E., Pecin, D., Pessoa, A., Poggi, M., Vidal, T., and Subramanian, A. (2017). New benchmark instances for the capacitated vehicle routing problem. *European Journal of Operational Research*, 257(3):845–858.

Wouda, N. A., Lan, L., and Kool, W. (2024). PyVRP: a high-performance VRP solver package. *INFORMS Journal on Computing*.

Yelmewad, P. and Talawar, B. (2021). Parallel version of local search heuristic algorithm to solve capacitated vehicle routing problem. *Cluster Computing*, 24(4):3671–3692.